

Multispectral estimation of retinal photoreceptor inputs

Salvador Bará,^{*1} Maria Angeles Bonmati-Carrion,^{2,3} Juan Antonio Madrid,^{2,3} Maria Angeles Rol,^{2,3} and Jaime Zamorano⁴

¹Dept. Física Aplicada, Universidade de Santiago de Compostela, 15782 Santiago de Compostela, Galicia

²Chronobiology Lab, Department of Physiology, College of Biology, University of Murcia, Mare Nostrum Campus, IUIE, IMIB – Arrixaca, Spain

³Fragilidad y Envejecimiento Saludable (CIBERFES), Madrid, Spain

⁴Dept. Física de la Tierra y Astrofísica, Instituto de Física de Partículas y del Cosmos (IPARCOS), Universidad Complutense de Madrid, 28040 Madrid, Spain

Received July 19, 2019; accepted September 25, 2019; published September 30, 2019

Abstract—Integrated multispectral devices provide convenient means for assessing the inputs to the five known photoreceptors present in the human retina. These photoreceptors drive relevant visual and non-visual pathways that control key aspects of human physiology. In this Letter we show that standard metrics of retinal photoreceptor exposure can be quantitatively estimated, to within a 5%, by means of 12 multispectral channels, 20 nm wide (FWHM), distributed across the visible range.

The key role of periodic cycles of light and darkness for regulating relevant aspects of human physiology is nowadays the subject of an intense interdisciplinary research effort, given its direct implications for human wellbeing and indoor/outdoor lighting design. Two recent breakthroughs provided a sound mechanistical basis for analyzing how the lit environment interacts with human health. One of them was elucidating several basic molecular mechanisms controlling circadian rhythms, for which Jeffrey C. Hall, Michael Rosbash and Michael W. Young were awarded the Nobel Prize in Physiology or Medicine 2017. Another one was the discovery in 2002 of a new type of retinal photoreceptor (the intrinsically photosensitive retinal ganglion cells, ipRGC) expressing the photopigment melanopsin [1], and directly signalling those brain structures that control daily rhythms.

The current consensus in this field is that non-visual effects of light acting through retinal paths for light detection and phototransduction rely on five specific spectral bands, corresponding to sensitivity of the S-, L-, and M-cones, the rods, and the ipRGC [2, 3]. These bands, depicted in Fig. 1, are commonly referred as cyanopic, chloropic, erythroptic, rhodopic, and melanopic channels, respectively.

Evaluating photoreceptor exposure in these bands is a requirement for quantitatively assessing the non-visual effects of light, both for basic, clinical, and population studies, and for the design and development of new

photonic lighting components and applications. Although retinal irradiance is strictly determined by the corneal spectral radiance and the spectral attenuation of the eye tissues [4], the current trend in experimental studies and theoretical phototransduction models formulation is using corneal irradiance as a proxy for determining retinal exposures [3, 5]. The reasons behind this extended practice are that corneal irradiance is easier to measure in most everyday life conditions than radiance, besides it provides a scaled and field-of-view averaged estimation of the actual retinal exposure.

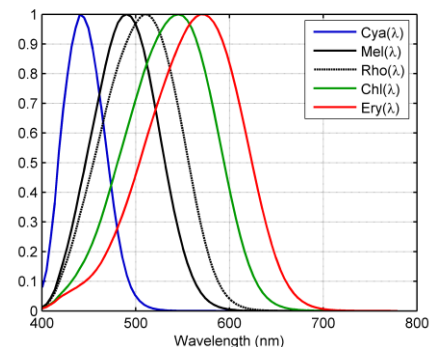


Fig. 1. Normalized spectral sensitivity bands of the five types of human retinal photoreceptors.

The spectral irradiance at the corneal vertex plane can be measured by standard spectrometric devices, from which band-weighted irradiances for each photoreceptor channel can be directly calculated. However, for large-scale monitoring of multiple spaces, it becomes necessary using smaller and cheaper devices, to estimate photoreceptor inputs with enough accuracy and precision.

An interesting technological option for gathering these exposure data is using off-the-shelf integrated photoelectronic devices acting as multispectral detectors. The irradiances detected in the available multispectral bands can be linearly combined with suitable weighting

* E-mail: salva.bara@usc.gal

coefficients, in order to obtain accurate photoreceptor input estimates. The optimum coefficients of these linear combinations can be determined by means of minimum variance estimators applied to the expected set of spectra to which persons will be exposed [4, 6], or, even more generally, by directly fitting in a least-squares sense the available multispectral sensitivity curves to the photoreceptor ones. The latter approach has the advantage of not requiring any *a priori* choice of an initial spectral set to build the exposure estimator.

The determination of direct fitting coefficients is straightforward. Denoting by \mathbf{p} the $N \times 1$ vector describing the spectral sensitivity curve of a given photoreceptor cell type, such that its generic i -th element, p_i , is the spectral sensitivity at wavelength λ_i , $i=1, \dots, N$, (Fig. 1), and denoting by \mathbf{A} the $N \times M$ matrix whose columns are formed by the values of the spectral sensitivity of the M spectral channels evaluated at the same discrete array of wavelengths $\{\lambda_i\}$, the optimum fitting coefficients \mathbf{c} , in the least-squares sense, form a $M \times 1$ vector that can be obtained as $\mathbf{c} = \mathbf{A}^+ \mathbf{p}$, where \mathbf{A}^+ is the Moore-Penrose pseudoinverse of \mathbf{A} [7], which can be computed using different standard algorithms generally included in most available calculation software packages, or directly as $\mathbf{A}^+ = (\mathbf{A}^T \mathbf{A})^{-1} \mathbf{A}^T$, where the superscript T stands for 'transposed', provided $\mathbf{A}^T \mathbf{A}$ is non-singular.

This in-band irradiance estimation procedure, commonly referred to in astrophysics as 'synthetic photometry', allows computing photoreceptor inputs as \mathbf{c} -weighted linear combinations of the signals recorded in the M multispectral channels. An example of design is shown in Fig. 2, where the first twelve channels of an off-the-shelf 18-band multispectral device (AS7265 by ams AG, Premstaetten, Austria), distributed across the visible range and with FWHM of 20 nm, are used to fit the five human photoreceptor bands. These twelve channels provide an adequate coverage of the spectral region relevant for this application.

It must be noted that these fits are not exact, as some residual ripples appear in the synthetic bands. This happens because the photoreceptor curves cannot be analytically expressed as exact linear combinations of the multispectral set of curves featured by this particular device. However, these ripples have minor consequences for estimating photoreceptor inputs under realistic exposure conditions. For most continuous spectra of practical interest, the effect of the ripples cancels out when performing the integral of the band-weighted irradiance. This can be checked by comparing the exact in-band irradiances with those that would be obtained using the fitted curves, for different incident light fields.

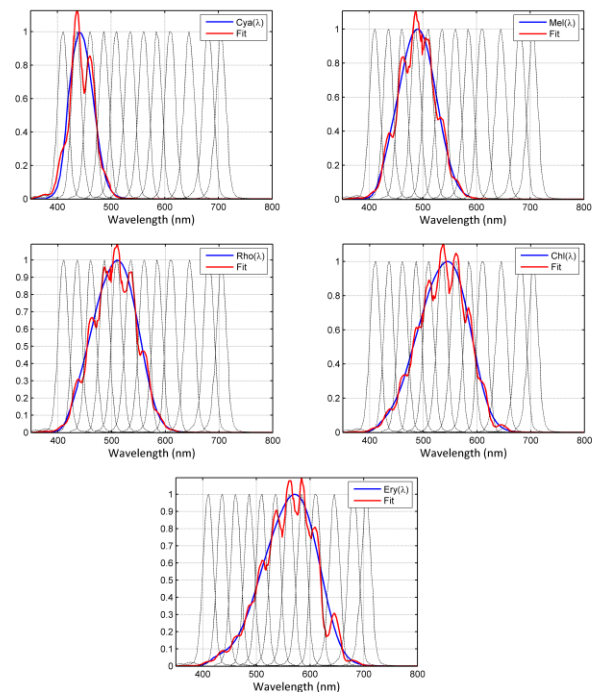


Fig. 2. Spectral sensitivity curves for synthetic photometry of the five human photoreceptor bands using a 12-band multispectral device.

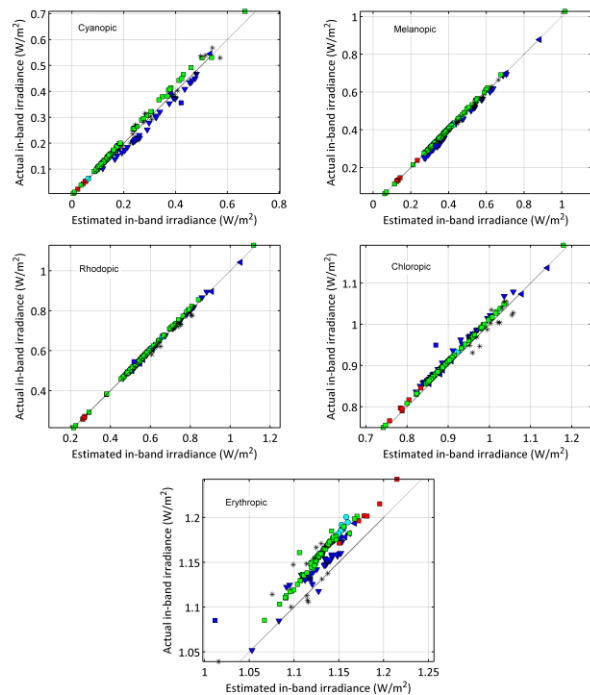


Fig. 3. Actual vs estimated in-band irradiances for 205 lamp spectra. Lamp types: halogen (\blacktriangle), incandescent (\bullet), high-pressure sodium (\blacksquare), LED (\blacksquare), fluorescent (\blacktriangledown), ceramic metal-halide (\blacklozenge), metal halide (\blackast), mercury vapor (\blacksquare).

Figure 3 shows the expected actual vs estimated irradiances in the five photoreceptor bands when direct light from a set of lamps of widely used technologies reaches on the corneal vertex plane a normalized illuminance of 683 lx. A total of 205 lamp spectra were used to compute these plots, comprising compact fluorescent, metal halide, ceramic metal-halide, T-type fluorescent, halogen, high-pressure sodium vapour, incandescent, light-emitting diodes with CCT in the range 1900÷7400 K, and mercury vapor lamps available on the market. The detailed characteristics of this lamp dataset can be found in reference [4].

The dotted straight lines are not fit lines but correspond to the exact 1:1 estimation. The residual relative estimation errors are reasonably small, averaging out at 5%, 1.8%, 1%, 1.2% and 2.3%, in absolute values, for the cyanopic, melanopic, rhodopic, chloropic and erythroptic bands, respectively. Note that the axes in the erythroptic plot (Fig. 3, bottom row) span a reduced range of values, in comparison with the other photoreceptor channels.

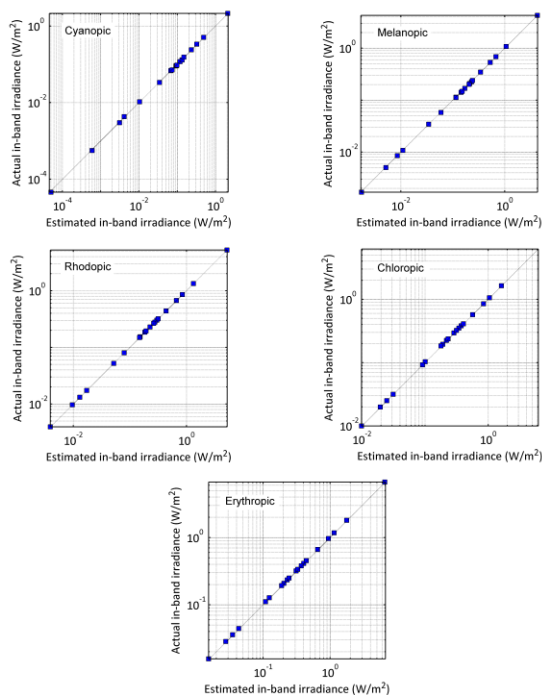


Fig. 4. Actual vs estimated in-band irradiances for 20 irradiance distributions recorded at homes or workplaces at different times of the day and with a different spectral source composition.

The residual estimation error can be expected to decrease when measuring actual irradiances occurring in everyday life settings as e.g. residential or workplace spaces. The reason is that for indoor spaces the light from the sources reaches the observer's eyes through many different propagation paths, including multiple reflections in the surrounding surfaces [8], generally leading to

smoother spectra. These smoothed spectra can be expected to be highly effective for cancelling out the effects of the residual rippling of the bands after the weighted integrations required to evaluate the photoreceptor inputs are carried out. A similar effect happens when averaging large datasets of exposures in outpatient studies.

Figure 4 shows the actual vs estimated irradiance for 20 different spectral irradiance distributions recorded at homes and workplaces using a Stellarnet BW-VIS-25 spectrometer. These spectra contain variable mixes of outdoor light, LED and fluorescent sources, and optoelectronic displays, reaching the observer's eyes directly and after multiple reflections at the walls. The axes are drawn in logarithmic scale to encompass the high dynamic range of the recorded signals. The residual relative estimation errors are of the same order but smaller than for the bare lamp spectra, averaging now to 3.2%, 1.6%, 0.8%, 1.7%, and 2.2%, in absolute values, for the cyanopic, melanopic, rhodopic, chloropic and erythroptic bands, respectively.

In conclusion, off-the-shelf integrated multispectral devices can be a useful tool for assessing human photoreceptor exposures relevant for evaluating visual and non-visual effects of light. The prospect of an easy availability of these data opens the way to implement optoelectronic systems for closed-loop monitoring and control of the artificially lit environment to which humans are exposed in a variety of everyday settings.

This work was supported by Xunta de Galicia/FEDER, grant ED431B 2017/64 (SB), the Ministry of Economy and Competitiveness through a CIBERFES grant (CB16/10/00239), 19899/GERM/15 from Fundación Séneca, and the Ministry of Science Innovation and Universities RTI2018-093528-B-I00 (all of them co-financed by FEDER) (JAM, MAR). Fundación Séneca's Research fellowship 20401/SF/17 to MAB-C. JZ acknowledges the support from ACTION, a project funded by the European Union H2020-SwafS-2018-1-824603, and RTI2018-096188-B-I00.

References

- [1] D.M. Berson, F.A. Dunn, M. Takao, *Science* **295**, 1070 (2002).
- [2] R.J. Lucas et al. *Trends Neurosci.* **37**, 1 (2014).
- [3] Commission Internationale de l'Éclairage, *TN 003:2015 Report on the First International Workshop on Circadian and Neurophysiological Photometry, 2013*. CIE, 2015.
- [4] A. Sánchez de Miguel et al., *J. Imaging* **5**(4), 49 (2019).
- [5] M.S. Rea, M.G. Figueiro, A. Bierman, R. Hamner. *Lighting Res. Technol.* **44**, 386 (2012).
- [6] D. Cao, P.A. Barrionuevo, *Chronobiol. Int.* **32**(2), 270 (2015).
- [7] P.B. Liebelt, *An Introduction to Optimal Estimation* (Reading, MA, Addison-Wesley, 1967).
- [8] J. Escofet, S. Bará, *Lighting Res. Technol.* **49**, 481 (2017).